*Carnegie Observatories Astrophysics Series, Vol. 3:*
*Clusters of Galaxies: Probes of Cosmological Structure and Galaxy Evolution, 2004*
*ed. J. S. Mulchaey, A. Dressler, and A. Oemler (Pasadena; Carnegie Observatories:*
*http://www.ociw.edu/ociw/symposia/series/symposium3/proceedings.html)*

# *XMM-Newton* Observations of the Poor Cluster MKW 4

E. O'SULLIVAN
*Smithsonian Astrophysical Observatory*

**Abstract**

We present a 15 ksec observation of the poor cluster MKW 4. While the cluster itself appears to be relaxed with little X-ray substructure, it is dominated by NGC 4073, a cD galaxy with a kinematically distinct core. We investigate the structure and properties of the cluster halo with particular reference to the temperature and abundance distribution of the gas and find that despite a declining central temperature profile and short cooling times in the core, there is no significant cooling flow.

## 1.1 Introduction

MKW 4 is a poor cluster or rich group first identified by Morgan, Kayser & White (1975) as part of their sample of cD galaxies in poor clusters. It contains $\sim$50 galaxies and is dominated by the cD/E galaxy NGC 4073. Kinematic studies of the galaxy population show the galaxies to be fairly evenly distributed about their mean redshift of $z$=0.02, with no sign of substructure (Koranyi & Geller 2002). There is some sign of spectral segregation, with absorption line galaxies more commonly found toward the centre of the group.

MKW 4 has been the subject of X–ray studies using *Einstein*, *ASCA* and *ROSAT*, all of which have shown it to be a fairly relaxed system (dell'Antonio, Geller & Fabricant 1995; Jones & Forman 1999), reasonably well modeled by at most two Beta models (Helsdon & Ponman 2000). The group X–ray halo has a mean temperature of $\sim$1.7 keV, placing it at the upper end of the group $L_X$:$T_X$ relation. Radial temperature profiles show that the temperature increases from $\sim$1.3 keV in the core, to a peak above 2.5 keV at $\sim$115 kpc and then drops back to a fairly constant temperature of $\sim$1.5 keV at higher radii. The *ASCA* data have been used to produce radial abundance profiles (Finoguenov, David & Ponman 2000), which show Fe, Si and S abundances which fall from central values of 0.4-0.7$Z_\odot$ to 0-0.2$Z_\odot$ at a radius of 500 kpc. We adopt a distance to MKW 4 of 79.945 Mpc, meaning that $1' =$ 23.255 kpc. We assume $H_0$=75 km s$^{-1}$ Mpc$^{-1}$ throughout.

## 1.2 Results

MKW 4 was observed with *XMM-Newton* during orbit 373 (2001 December 21) in two exposures of $\sim$16000 and $\sim$4500 seconds. The EPIC MOS and PN instruments were operated in full frame and extended full frame modes respectively, with the medium filter. Using the XMM Science Analysis Software (SAS V.5.3.3) we filtered the data to remove bad pixels and columns, X-ray events not corresponding to patterns 0-12 for the two MOS cameras and patterns 0-4 for the PN camera, and a short flare at the beginning of the observation. The effective exposure times for the MOS and PN cameras were 14.1 and 10.5 ksec, respectively.

### *1.2.1 Surface Brightness Models*

In order to model the surface brightness distribution, we produced images for use in the CIAO SHERPA fitting software. Using data for all three EPIC cameras we searched for and removed all point sources, except the false identification of the core of the diffuse emission. We also produced background data sets based on the blank-sky data of Lumb (2002), using the 'double-subtraction' technique (Arnaud et al. 2002; Pratt, Arnaud & Aghanim 2001).

We initially attempted to simultaneously fit these images with a variety of model combinations (*e.g.* single beta model, beta+beta, beta+point source, *etc.* ). However, none of these models was successful in fitting the halo as a whole, so we decided instead to model sectors of the halo individually. We selected four sectors, covering the major and minor axes of the halo. The NW and SE sectors showed deviations from a simple beta model, with the NW sector showing emission extending to higher radii, and the SE sector showing a 'bulge' of excess emission at $\sim$20 kpc. The two remaining sectors were well described by a single beta model and had similar core radii and slopes, leading us to fit them together. Taking into account the effect of the PSF and excluding all data outside the NE and SW sectors, we found the best fit to be a beta model with a core radius of $10.02^{+2.87}_{-3.16}{}''$ (equivalent to $3.88^{+1.11}_{-1.22}$kpc) and $\beta_{fit}$=$0.457^{+0.017}_{-0.015}$ (1 $\sigma$ errors).

### *1.2.2 Temperature and Abundance Profiles*

In order to examine the large scale temperature and abundance structure of the group we produced radially binned spectra of the halo. All data within 17$''$ of point sources were removed and spectra were fit using an absorbed MEKAL model in a 0.4-4 keV energy band. Figure 1.1 shows the results of our fits.

The temperature profile shows a fairly smooth decline in temperature towards the core, consistent with *ROSAT* results (Helsdon & Ponman 2000). Metal abundance is strongly affected by changes in hydrogen column. The fit quality in the central bins is poor, and we experimented with different models to fit these bins. The fits could be improved by using a two-temperature model, but the higher temperature component was never well constrained by the data. Using cooling flow models did not produce good fits except in cases where the emission from low temperature gas (*i.e.* gas at temperatures lower than $\sim$ 1 keV) was minimal. We also used a deprojection model to take account of the multiple temperatures of gas along the line of sight, but found only small differences between the projected and deprojected profiles.

Using the VMEKAL model in *xspec* we are able to fit Fe, Si and S individually, as well as the abundance of remaining metals and the temperature in each bin. Figure 1.2 shows abundance profiles for Fe, Si and S, shown with reference to the profile for all other metals combined. There is a clear increase in all three elements in the core of the group, at the location of NGC 4073

### *1.2.3 3-D Gas Models*

Using software provided by S. Helsdon, we use the surface brightness fit derived in Section 1.2.1 and the radial temperature profile shown in Figure 1.1 to calculate quantities such as gas mass, total mass, gas cooling time and gas entropy for the inner region of the

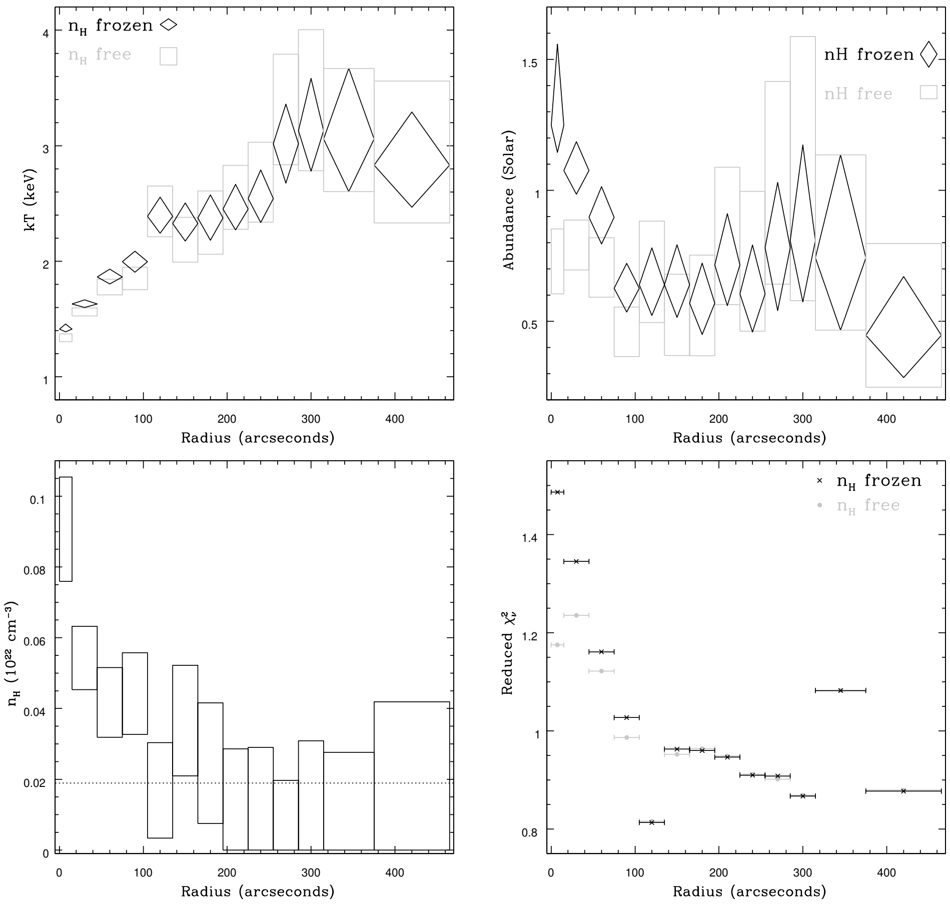


Fig. 1.1. Projected temperature, metal abundance and absorption profiles for MKW 4, with fit statistic for each bin. In the temperature and abundance plots, diamonds show 90% limits on fits in each annulus with $N_H$ frozen at the galactic value. Rectangles show the limits on fits with the hydrogen column free to vary. The $N_H$ plot has the galactic absorption value marked at as a dotted line, while the rectangles show the 90% limits for each annulus when $N_H$ is fit. In the fit statistic plot, the reduced $\chi^2_\nu$ of the fit with $N_H$ frozen is shown by crosses, and with circles for fits with $N_H$ free.

group. The software infers the gas density profile based on the fitted surface brightness profile and a model description of the temperature profile, and normalises it by comparison with the X–ray luminosity. Given this density profile we can use the well known equation for hydrostatic equilibrium to calculate the total mass at any given radius. Entropy is defined as $S = T/n_e^{\frac{2}{3}}$. Figure 1.3 shows radial profiles for these parameters, as well as gas fraction.

For comparison with other systems, we use an estimate of $R_{200}$=973 $h_{75}$ kpc (the radius at which the system has a density of 200 times the critical density of the universe, approximately equal to the virial radius) based on fits to *ROSAT* data (Helsdon & Ponman 2000).

Total mass and entropy seem quite comparable to systems of similar X–ray temperature (Nevalainen, Markevitch & Forman 2000;Lloyd-Davies, Ponman & Cannon 2000). Gas

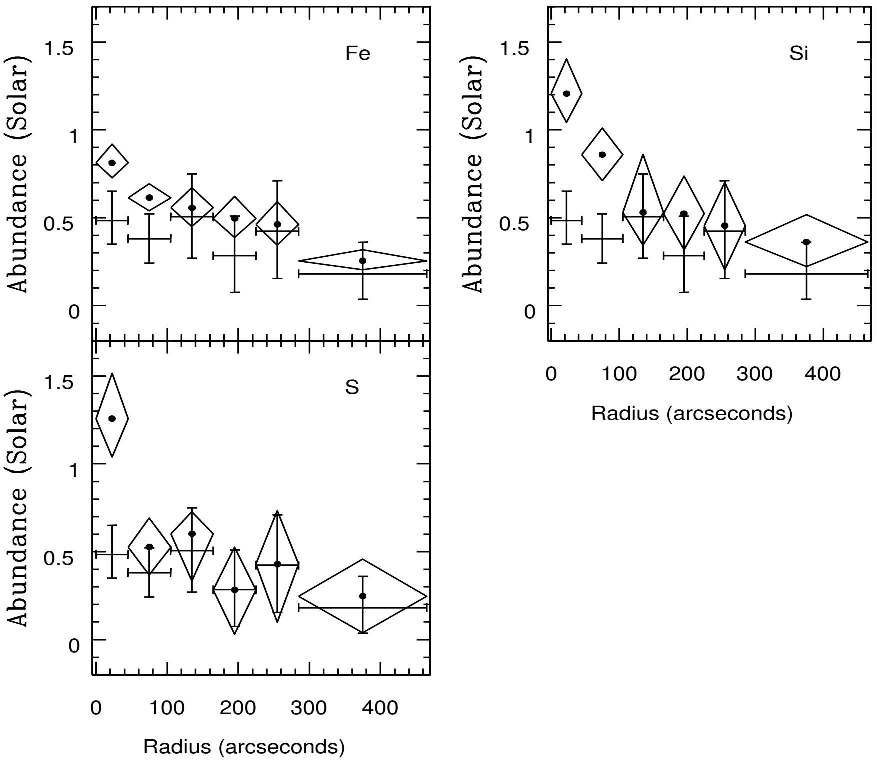


Fig. 1.2. Radial abundance profiles for Fe, Si and S. In each plot, diamonds show the 90% error on the metal in question, as labeled on the plot. The crossed error bars show the fit to all the remaining metals, again with 90% errors. $N_H$ was fixed at the galactic value in all fits.

mass appears at first glance somewhat low, but comparison with other cool systems (Sanderson et al. 2003) suggests that this value may not be unrealistic, given the low fraction of the virial radius to which we can measure. There is no central isentropic core in the group. Some models of entropy injection in galaxy groups and clusters predict a flattening of the entropy profile in the cores of the systems (*e.g.* Muaonwong et al. 2001; Tozzi & Norman 2001), but this is clearly not the case in MKW 4

## 1.3 Conclusions

Based on our results we conclude that:

(1) Although the surface brightness distribution shows signs of some disturbance along a NW-SE axis, the group has not undergone any significant merger in the recent past. There is no evidence of past or ongoing AGN activity.

(2) We see evidence of enhanced metal abundance in the gas in the core of the group. This enrichment is likely caused by supernovae in the dominant galaxy, NGC 4073.

(3) The group has a steep temperature profile and the gas cooling time in the core is short. However, our most successful spectral fits indicate that there is little or no gas below a temperature of $\sim$1 keV, indicating that only small amounts of gas can be cooling out of the X-ray regime, even in the core of the group. Given the lack of evidence for shocks or

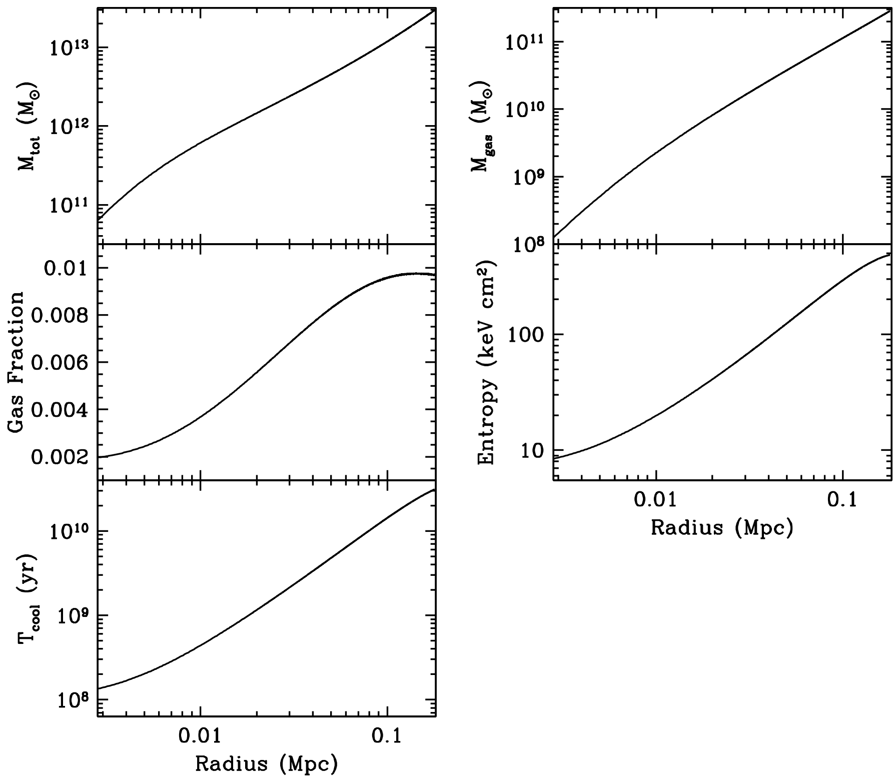


Fig. 1.3. Radial profiles of total mass, gas mass, gas fraction, entropy and cooling time, for the inner regions of the MKW 4 group.

AGN activity capable of heating the gas, we must assume that MKW 4 is in the process of establishing (or re-establishing) a cooling flow.

This work was supported by NASA grants NAG5-10071 and GO2-3186X.

## References


Arnaud, M. et al. 2002, A&A, 390, 27

dell'Antonio, I. P., Geller, M. J. & Fabricant, D. G. 1995, AJ, 110, 502

Finoguenov, A., David, L. P. & Ponman, T. J. 2000, ApJ, 544, 188

Helsdon, S. F. & Ponman, T. J. 2000, MNRAS, 315, 356

Jones, C., & Forman, W. 1999, ApJ, 511, 65

Koranyi, D. M. & Geller M. J. 2002, AJ, 123, 100

Lloyd-Davies, E. J., Ponman, T. J. & Cannon, D. B. 2000, MNRAS, 315, 689

Lumb, D. 2002, EPIC background files, http://xmm.vilspa.esa.es/docs/documents/CAL-TN-0016-2-0.ps.gz

Morgan, W. W., Kayser, S. & White, R. A. 1975, ApJ, 199, 545

Muanwong, O., Thomas, P. A., Kay, S. T., Pearce, F. R. & Couchman, H. M. P. 2001, ApJ, 552, L27

Nevalainen, J., Markevitch, M., & Forman, W. 2000, ApJ, 532, 694

Pratt, G. W., Arnaud, M. & Aghanim, N. 2001, in Clusters of Galaxies and the High Redshift Universe Observed in X-rays, ed. Neumann, D. M. & Tranh Thanh Van, J. (in press)

Sanderson, A. J. R., Ponman, T. J., Finoguenov, A., Lloyd-Davies, E. J. & Markevitch, M. 2003, MNRAS, 340, 989

Terlevich, A. I. & Forbes, D. A. 2002, MNRAS, 330, 547

Tozzi, P. & Norman, C. 2001, ApJ, 546, 63